

NASA Contractor Report 187148

1N20
157896
P.50

Solar Concentrators for Advanced Solar-Dynamic Power Systems in Space

Study Final Report

Richard Rockwell
Hughes Danbury Optical Systems, Inc.
Danbury, Connecticut

(NASA-CR-187148) SOLAR
CONCENTRATORS FOR ADVANCED
SOLAR-DYNAMIC POWER SYSTEMS IN
SPACE Final Report (NASA) 50 p

N93-23017

Unclass

G3/20 0157896

March 1993

Prepared for
Lewis Research Center
Under Contract NAS3-25280

NASA
National Aeronautics and
Space Administration

TABLE OF CONTENTS

Summary	4
I. Introduction	6
II. Requirements	8
III. Thermal / Structural Analysis	10
IV. Panel Design and Fabrication	13
V. Testing	16
VI. Conclusions	19
Tables	20
Figures	23
References	48

LIST of TABLES

Table 1	Generic design honeycomb panel construction used for thermal analyses	20
Table 2	Thermal analysis assumptions (properties)	21
Table 3	Pre- and post- thermal cycling radius and slope measurement results for spherical panels	22

LIST of FIGURES

Figure 1	Baseline panel design description	23
Figure 2	Typical glass - composite facesheet lamination sequence	24
Figure 3	Typical panel assembly sequence	25
Figure 4	Thermal analysis model network diagram	26
Figure 5	Unit cell model for analysis of structural behavior	27
Figure 6	Effect of coating location on steady state panel temperatures	28
Figure 7	Effect of rear surface emittance on steady state panel temperatures for back-coated facesheet.	29
Figure 8	Effect of rear surface emissivity on steady state panel temperatures for front-coated facesheet.	30
Figure 9	Orbital transient panel temperatures for back-coated glass	31
Figure 10	Orbital transient panel temperatures for front-coated glass	32
Figure 11	Front-to-back temperature gradient for back-coated panel	33
Figure 12	Front-to-back temperature gradient for front-coated panel	34
Figure 13	Through the thickness temperatures for back-coated panel	35
Figure 14	Through the thickness temperatures for front-coated panel	36
Figure 15	Orbital transient panel temperatures as a function of total surface emissivity using closed form analysis	37
Figure 16	Effect of adhesive fillet size on panel surface deformations due to adhesive cure shrinkage	38
Figure 17	Effect of adhesive fillet size on panel surface deformations due to temperature changes	39
Figure 18	Effect of adhesive fillet size on facesheet 'effective CTE' as a function of fillet size and substrate CTE.	40
Figure 19	Point design panel description	41
Figure 20	Design of composite laminate to match required CTE	42
Figure 21	Coupon tests of substrate CTE for chosen laminate design	43
Figure 22	Atomic oxygen erosion tests of candidate adhesives	44
Figure 23	Coupon surface distortion before and after thermal cycling	45
Figure 24	Diagram of test station to measure radius of curvature and integrated (rms) slope error	46
Figure 25	Typical image spot from spherical panel and intensity scan	47

SOLAR CONCENTRATORS FOR ADVANCED SOLAR-DYNAMIC

POWER SYSTEMS IN SPACE

Richard Rockwell
Hughes Danbury Optical Systems
Danbury, CT 06810

SUMMARY

This report summarizes the results of a study performed by Hughes Danbury Optical Systems (formerly Perkin-Elmer Corp) to design, fabricate, and test a solar concentrator panel concept suitable for use in space using microsheet glass as the top layer of an otherwise composite panel. This approach leads to a reflector panel which achieves the high specularity and durability of an all glass mirror without the weight penalty. At an areal density of 2 kg/M^2 the resultant panel's weight is equivalent to a mere 0.03 inches of glass.

This study is a follow-on activity to an earlier NASA funded study which demonstrated the manufacturability of such a design. In the earlier study the substrate material (Kevlar) was arbitrarily chosen for convenience and only cursory testing was performed. The current study looks critically at the design of the panel and selection of materials for durability and includes quantitative measures of performance.

Two variations of this design were considered. As a second surface reflector (coating on the back of the glass layer) the panel would likely be very resistant to environmental forces in low earth orbit since it's reflective layer is beneath a relatively thick protective layer of glass. As a first surface reflector (coating on the front of the glass) the panel will show better structural durability since the glass can be bonded directly to the composite substrate, that is, without concern for the reflective coatings. The first surface reflector option was chosen as the better approach based on a analysis of operating temperatures in low earth or geosynchronous orbit. The second surface reflector, with it's high emissivity glass layer on top would run so cold as to make condensation and contamination problem.

Thermal and structural modeling was done to determine the appropriate design parameters for the panel. The resultant design uses a composite substrate designed to have a coefficient of thermal expansion very near that of the glass layer. This was done primarily to minimize the effect of orbital temperature variations on curvature and slope error. Analysis also dictated that the adhesive bond between the honeycomb core and facesheet of the panel have fillets of minimum size.

After satisfactory test of components and flat test coupons spherically curved panels approximately 12 inches in diameter and with a radius of curvature of 10 meters (394 inches) were built, coated, and thermally cycled. Tests on the curved panels was limited to thermal cycling since it was thought to be the most likely source for problems. Also, component tests performed earlier were thought to adequately assess the design's resistance to atomic oxygen and particulate erosion. Measurement of the pre- and post-cycling surface shape of the curved panels produced two notable results. First, the initial radius of curvature of the panels was not maintained through coating and thermal cycling. Thermal creep of the epoxy adhesive is thought to be the problem. Second, after accounting for the radius change, the rms slope error appears to change only slightly. This point is encouraging in that the fundamental design of glass on composite appears to be viable if the radius change problem can be solved.

I. INTRODUCTION

Solar concentrator panels for use in space, whether in high or low orbit, must provide and maintain a high geometric accuracy and a high quality reflective surface throughout their life. Since weight is a critical concern for such concentrators, the panels must be as light as possible with 2 kg/M^2 being accepted as a reasonable areal density goal. If weight was not a concern the material of choice would likely be glass because of its inherent resistance to environmental degradation and smooth (specular) surface. To meet the need for a smooth durable surface without the weight penalty of an all glass reflector an approach has been under study which uses microsheet glass (0.009 inches thick) as the top layer of a lightweight composite honeycomb panel. This approach was originally proposed as a second surface reflector with the reflective coatings on the back surface of the glass where it would be protected from degradation. The potential feasibility of a glass-composite approach was demonstrated previously in a NASA funded study. Details can be found in the NASA Contractor Report entitled 'Lightweight Solar Concentrator Panel for Space Applications' dated July 1998 (ref 1).

In the previous study the panel design, shown in figure 1, was chosen because of material availability and familiarity with its fabrication techniques. The high susceptibility of Kevlar to the atomic oxygen in low earth orbit is well known but it provided an adequate and available testbed for a demonstration of the glass-composite panel fabrication techniques. The current study was more rigorous in that analyses and tests were performed to select and verify an appropriate panel construction. The basic approach is to co-cure the microsheet glass to the composite facesheet prior to assembling the honeycomb sandwich panel. A typical glass-composite facesheet layup is shown in figure 2. The best results were achieved when the glass-composite facesheet was laminated over a spherical mold. The glass is cold formed (strained) to the spherical shape and ultimately held in that geometry by the composite honeycomb sandwich. Figure 3 outlines the sandwich assembly.

The scope of this study was to analyze, design, and test the glass-composite panel approach using materials, processes, and construction selected specifically for this application. The design goals are:

- 1) Areal density of 2 kg/sq meter
- 2) Surface integrated slope error ≤ 1 milli-radian

II. REQUIREMENTS

The design considerations for the concentrator panel cover a broad range of issues which are derived from its intended use in the concentrator for a high temperature solar dynamic power system. The requirements fall into two categories, those which are generic to solar concentrators and those which are specific to the glass-composite panel approach (ie, imposed and derived). The generic requirements are briefly stated below and are more fully described in the earlier study report.

SURFACE ACCURACY: To achieve high temperatures at the receiver, the concentrator must operate at a concentration ratio over 2000 with an intercept factor exceeding 90%. An 'as-manufactured' surface accuracy of approximately 1.0-2.0 milli-radians at one sigma is required to achieve the high concentration ratio.

REFLECTIVITY: To minimize the required collector area, the surface must reflect a high percentage of the total incident solar flux (e.g. 88% or more). For solar power generation the relevant criteria is the 'integrated reflectivity' which accounts for properties of the reflective surface as well as the source, considering the wavelength dependence of both solar flux and reflectivity. For any particular panel configuration, reflectivity will be primarily a function of the coating material and its method of application.

SPECULARITY: In addition to being highly reflective, the concentrator's surface must be highly specular (as opposed to diffuse) to ensure that a high percentage of the reflected energy is directed to the receiver. The specularity of a reflective surface is driven by the roughness (and micro-roughness) of the substrate and accounts for irregularities whose length scales range from sub-micron to several angstroms.

ENVIRONMENTAL DURABILITY: The initially high performance of the concentrator must be maintained for a period of 10 years or more. Therefore, the design must account for the performance degrading influence of atomic oxygen, ultra-violet light, micrometeorites, space debris, and thermal cycling. This is

especially true for the reflective coatings since they are typically less than a half micron thick at the start.

WEIGHT: Weight is critical for any flight hardware. This is especially true for solar concentrators since a flight system may contain thousands of square meters of collector area. A goal of 2kg/M^2 is consistent with the ongoing Space Station development efforts.

MANUFACTURABILITY: The high costs for producing high accuracy concentrator surfaces precludes any grinding or polishing of the as-manufactured panel. Alternative and cost effective methods must be selected for production of optical surfaces. As such, the approach described herein is not applicable to materials such as aluminum.

Additionally, the glass-composite panel design approach leads to another set of requirements relating to the thermal-mechanical behavior of the panel as described below.

SURFACE QUILTING DEFORMATIONS: Since the panel is incorporates a honeycomb sandwich core, the fabrication process can have tendency to leave a print-thru of the honeycomb core on the front face. This print-thru results primarily from the effects of the adhesive fillets used to bond the facesheet to the honeycomb core. Analyses described elsewhere in this report show clearly that low surface quilting requires fillets of minimum size or increased thickness of the front face of the panel.

COMPOSITE MATERIAL CTE: Mismatch in the coefficient of thermal expansion between the glass layer and composite facesheet can lead to both surface quilting (print-thru) and high stresses in the glass. Analyses described elsewhere indicate that the composite facesheet's CTE should be in the range of 3.5 to 4.5 ppm/°F.

OPERATING TEMPERATURE: The average operating temperature of a concentrator panel can be altered by use of appropriate thermal control coatings.

The desired temperature is a range above that at which condensation will occur but below the limits of the materials used.

III. THERMAL AND STRUCTURAL ANALYSES

Thermal and structural analyses were performed on a generic panel configuration to determine appropriate design values for the point design. An analysis of the generic design with typical properties was used to get the broadest possible understanding of the parameters which affect the design from the limited program funds. The generic design is a honeycomb sandwich panel with a hexagonal core and composite face sheets. Separate models were used for thermal and structural analysis. For each, the model represents a unit cell (one hexagon of the honeycomb core) and includes appropriate boundary conditions to represent the surrounding cells

The thermal model, described schematically in figure 4, includes both conductive and radiative couplings within the panel. Material properties and design assumptions are listed in tables 1 and 2. The model consists of a series of simultaneous equations which are solved using TKSolver for the IBM PC. This modeling approach, rather than using the more conventional SINDA thermal analysis program, allowed us to parametrically vary the input parameters and identify design drivers. Outputs from the thermal modeling analyses include mean operating temperatures, gradients, and transient orbital temperatures for a wide range of design parameters. Results from these analyses were used to select appropriate thermal control coatings, materials, and geometry.

The structural model, shown in figure 5, is an axisymmetric model of a unit cell with appropriate boundary conditions to reflect the surrounding cells. The model is made using the NASTRAN finite element code running on an IBM mainframe computer. It includes the glass facesheet, composite facesheets, honeycomb core, glass/composite adhesive layer, and fillet bonds between the core and facesheets. The model was run for various values of CTE of the facesheets, and adhesive fillet size. The main outputs were stresses in the glass and composite layers, adhesive induced surface quilting deformations, and thermally induced deformations.

The following paragraphs present the results of the thermal and structural modeling and their interpretation with respect to the panel design.

Thermal Analysis Results

A parameter that proved critical to the design was whether the glass was coated with the reflective film on its back face (second surface reflector), as in the earlier study, or on the front face (first surface reflector). For the case of steady state solar viewing (as in GEO) the effect of coating location on the average operating temperature was shown to be as high as 375°F (210°C). This assumes a solar absorptance of 10% and a varying panel rear surface emissivity as shown in figure 6. The large difference in average temperature is a result of the vastly different surface emissivity on the front and back coated glass. The back coated glass has a high thermal emissivity making it act much like the optical solar reflectors (OSR) used to achieve high ratios of absorptance to emissivity to cool GEO based satellites. Figures 7 and 8 expand upon the trend of figure 6 to show the effect of a change in solar absorptivity over life.

For the case of low earth orbits, the variation of temperature when going from sun to shadow is as important, if not more so, than the average. Analyses were made of orbital transient temperature for both front and back coated glass as shown in figures 9 and 10. The orbital solar radiation considered 60 minutes of sun followed by 30 minutes of shadow. No provisions were made to account for earth albedo or radiation which might affect both the average and variability of temperature.

Also of interest for low earth orbit is the front to back thermal gradient of the reflector panel and the change in gradient with orbital position. Figures 11 and 12 show that the front coated glass approach provides a more constant temperature gradient through the thickness. This results from the overall lower surface emissivity of the front coated glass. The distribution of temperature through the panel cross section is shown in figures 13 and 14.

These parametric analyses lead to two conclusions. First, the back coated glass panel is unsuitable for either GEO or LEO applications due to its low operating temperature and the resultant risk of contamination from condensation. Second, the average operating temperature can be adjusted by selection of an appropriate rear

surface coating for the panel with low emissivity coatings yielding higher temperatures. For the case of low earth orbit, this trend is readily seen in the temperature plots in figure 15 which show temperature as a function of solar absorptance and surface emissivity. The case of an emissivity of 0.20 and absorptance of solar 15% was chosen as the design point because it provides high enough temperatures to prevent condensation but low enough to be compatible with the limits of the adhesives.

Structural Analysis Results

The main objectives of the structural modeling were to determine an appropriate design point for the CTE of the composite facesheet, to set a limit on the core to facesheet adhesive fillet size, and to ensure that the stress levels resulting from thermal cycling and fabrication temperatures do not fracture the glass. In the earlier study, it was noted that quilting of the reflective surface changed with temperature. To minimize this effect in the redesigned panel a study was made of the effect of fillet size on the surface deformations due to adhesive shrinkage and change in temperature.

For the case of adhesive cure shrinkage, a linear shrinkage rate of 1/2% was assumed. A thermal load was applied to the adhesive fillet to simulate the shrinkage. The plot in figure 16 shows the relationship between panel surface deformation and fillet size. Analysis of the distribution of displacement and slope error over the unit cell indicated that the rms slope error (1 sigma) was equal to the peak displacement times 15. If 0.5 milliradians slope error is allocated to the change in surface slope error due to adhesive shrinkage then the maximum surface displacement is of order 33.0×10^{-6} inches (1 micron). As shown in the plot, this criteria limits the fillet cross section to 0.018 inches

The effect of bulk temperature changes was modeled similarly with the results shown in figure 17. Based on an operating temperature which differs from the fabrication temperature by up to 400°F and the same 0.5 milliradian slope error allocation, the fillet size is shown to be limited to 0.010 inches. As expected, this case governs.

Based on a consideration of stresses in the glass layer it was determined that the CTE of the composite laminate used for the facesheet should be between 3 and 4 ppm/°F which is slightly below the glass CTE of 4.1 ppm. This results in tensile stress

in the glass at 0°F of less than 1000 psi. Figure 18 shows the effect of the adhesive fillets of the facesheet CTE. As expected, larger fillets (more high CTE adhesive) raises the CTE slightly.

IV. PANEL DESIGN AND FABRICATION

Based on the analyses discussed in section III, the requirements of section II, and the experience of the earlier study, the baseline panel was redesigned as shown in figure 19 and described below.

Corning's code 0211 microsheet glass with a thickness of 0.009 inches is bonded to the substrate. The glass is used as received except for cutting to size and cleaning. High surface specularity is ensured by it's fire polished finish .

The glass is bonded to a composite laminate using American Cyanamid's FM300 film adhesive with a an operational temperature limit of 450°F. The bonding is performed at the same time that the facesheet composite laminate is cured.

The facesheet laminate consists of alternating layers of 120 style E-glass and T300 graphite epoxy (934 resin system) with the E-glass making up 2/3 of the thickness. These materials and their relative thicknesses result from an analysis of the effective CTE of the laminate. As shown in figure 20, this ratio should yield a CTE of 3.75 ppm/°F. Three test coupons were made and tested for CTE. The resultant CTE's as shown in figure 21 were consistently on the high side but were deemed acceptable for continued development.

The honeycomb core is aluminum rather than E-glass as was assumed in the analyses due to the unavailability of small quantities of E-glass honeycomb. The aluminum core (3/16 in cell, 0.001 in wall, 0.25 in thick) should lessen front to back thermal gradients in the panel and make the bonding operations simpler with more uniform fillets. The facesheet laminates are bonded to the honeycomb core at room temperature using Hysol EA9394 adhesive with a service temperature rating of 450°F. Fillet size is minimized by troweling the adhesive onto a glass panel then rolling the honeycomb onto it. When the honeycomb is removed a small amount of adhesive adheres to the aluminum which is sufficient to bond the facesheets.

Fabrication of the panels is in two phases; preparation of the laminated face skins and bonding of the components into the completed panel. In the laminate phase the composite face skins are layed-up and cured. Vacuum bagging is used to remove any trapped air in the laminate and consolidate the layers. An over-pressure (autoclave) is also used to augment the consolidation and ensure conformance to the mold. In the bonding phase the laminated face skins are bonded to the honeycomb substrate using an over-press (mechanical clamping) and room temperature curing of the adhesive. All of the fabrication is done over a mold of the proper contour; flat or spherically convex depending on the desired panel shape. The fabrication steps which led to the highest quality panels are summarized as follows:

- 1) Apply chemical release agent (Frekote 44) to the surface of the spherical mold.
- 2) Cover mold surface with 120 weight peel ply cloth. This prevents sticking of the face skins to the mold.
- 3) Clean microsheet glass free of dust contamination and place on mold surface.
- 4) Apply one layer of American Cyanamid FM300 film adhesive to the back surface of the glass.
- 5) Lay down a single ply of 120 style E-glass cloth followed by a single ply of T300 graphite epoxy prepreg cloth then another ply of the E-glass using a 45/90/-45 orientation.
- 6) Vacuum bag mold and autoclave cure part using full vacuum (25 in. Hg) and 30 psi over-pressure. Cure cycle will be a 30 minutes rise to 350°F, hold for 90 minutes then release pressure but maintain vacuum until cool.
- 6a) Repeat steps 1,2,5, and 6 to form rear face-skin (no glass).

- 7) After curing, check glass for defects. Reposition cleaned front face-skin onto mold, glass side down, and hold in place with vacuum.
- 8) Using Hysol EA 9394 epoxy, wet both sides of a 0.25 inch thick Aluminum honeycomb core. Place core onto back surface of laminated face-skin.
- 9) Place the rear face-skin onto the outside surface of honeycomb core.
- 10) Apply mechanical pressure to the honeycomb sandwich with a spherical fiberglass overpress. Allow adhesive to cure for 12 hours at room temperature.
- 11) Trim excess core and laminate material from panel.

After the fabrication is completed the panels are cleaned and coated. Cleaning is accomplished via a solvent wash followed by 48 hours of vacuum outgassing and a second wash then a glow discharge cleaning just prior to deposition of the coating. While not directly influencing the performance of the panel, the reflective coating is applied to the glass face to enable testing. The coating applied to the glass face of the panel consists of:

- 1) a binder layer of Yttrium oxide to promote glass-silver adhesion
- 2) 2000 angstroms of Silver
- 3) 700 angstroms of Al_2O_3
- 4) 2200 angstroms of SiO_2

This coating is typical of the type proposed for the space station solar concentrator. Its durability is discussed by Gulino in reference 2.

V. TESTING

In addition to the coupon CTE measurements described earlier, at key points in the panel design and fabrication phase, testing was conducted to establish the behavior under selected test conditions. These tests and results are described in the following paragraphs.

Atomic oxygen erosion: Before committing to a particular adhesive, atomic oxygen erosion tests were performed at NASA Lewis Research Center to determine which candidate materials were best suited to the low earth orbit environment. Four adhesives were tested including a low and high temperature version of two types of adhesives used in the panel construction. They are American Cyanamid FM73 and FM300 , and Hysol EA956 and EA9394. The tests were performed by applying the adhesives to prepared stainless steel plates, curing the adhesive per specification, and exposing them to atomic oxygen in an Asher facility. The summary results are presented graphically in figure 22. Notably, the high service temperature adhesives (FM300 and EA9394) performed better than their lower service temperature counterparts. A two inch square section of a completed flat panel was also tested for atomic oxygen erosion. After the equivalent of 7.2 years in space the mass loss, a measure of erosion, was 3.2%. A more thorough discussion of the tests performed at NASA Lewis Research Center is available in reference 3.

Coupon surface quilting test: Before fabricating curved panels, several 2 inch flat panels were made and tested. Figure 23 shows a typical one dimensional profile of a typical section of the test coupon before and after 30 thermal cycles of 30°F to 195°F with 30 minutes residence at each endpoint. Although the scale of the plots is different it is clear that the peak to peak deformation was not significantly affected. This particular undulation is attributed to a print-thru of the fabric weave used in the facesheet laminate.

Temperature extremes: As a measure of durability one coupon was heated in an oven to 400°F to determine if any delamination or debonding occurred. Visual inspection yielded no evidence of damage, that is, no debonding or permanent deformation. No other measurements were made. A second coupon was rapidly cooled by immersing it in liquid nitrogen (77°K) and removed. Again, no visible damage.

Optical Testing

Testing of the spherically curved panels was performed by inserting the test panel into an optical path and recording the resultant image blur. The optical path consisted of a Helium Neon laser source and pinhole, a collimating mirror, test articles of various size (typically 12 inch diam), and a camera body as shown in figure 24. This approach was taken so that average radius and slope error (blur) could be assessed simultaneously. Since the two measurements are made simultaneously there is no cross coupling between radius and slope error, that is, slope error is measured at 'best focus'. Best focus is defined by minimum blur size.

A laser illuminated pinhole was placed at the focus of a high quality parabolic mirror which collimates the light. The source was off axis (approximately 5°) with respect to the parabola so the collimated beam was accessible. The test panel was then placed in the collimated beam and oriented to steer the reflected light back to the parabola which re-images the pinhole. If the test panel was perfectly flat, the image would fall back in the source and be of comparable size. Since the test panels are concave, the image of the pinhole fall short of the source. The location of the image defines the radius of curvature of the test panel. Additionally the image is blurred due to the slope errors on the test panel. A camera, with no lens, was placed at the blurred image to record the intensity distribution within the spot. The blurred image was then scanned using a micro-densitometer to determine the distribution of energy within the spot. Figure 25 shows a sample spot and the corresponding scan. As shown the distribution is nominally Guassian and thus rapidly falls to near zero at the 3 sigma width. This width corresponds roughly to the visually opaque edge of the blur spot.

Measurements were made before and after thermal cycling of the panels to determine to what extent the panels changed. Table 3 presents the resultant radii and slope errors for the tested panels. A total of five spherical panels were built, coated, and tested. The panels are in two groups: designations A, B, and C were for panels that were thermal cycled and designations 1 and 2 were for panels that were not thermally cycled.

To fully appreciate the data summarized in table 3, one needs to know more about the history of each panel. Panels A, B, and C were fabricated at the same time. They were formed on a mold with a 10.0 Meter radius of curvature. All three were then

coated and evaluated. No measurement of the radius or slope was made prior to coating. This would have required an alternative test setup since the panels are poor reflectors prior to coating. After coating, it was noted that the panels appeared quite flat as opposed to the curvature that existed prior to coating. It is not known when or why the panels flattened. The source is assumed to be thermally induced creep in the adhesive which bonds the core to the facesheets (Hysol EA9394). This is presumed to have happened during the glow discharge cleaning. Since the glass is cold formed to a sphere, stresses are locked into the panel during fabrication. Upon heating, the adhesive may have softened allowing the strain to partially relieve, thereby flattening the panel. Although the adhesive is rated for 450°F, creep is not precluded at lower temperatures. The 450°F value appears to be a strength criteria only. As shown, the nominal radius of all three panels is significantly different from that of the mold.

It was decided to continue with the thermal cycling tests anyway to learn what we could. Panel A was not cycled, panels B and C were cycled 400 times between 30°F and 195°F. The pre and post coat measurements indicate some change in the surface slope error of both panels, although both are less than the 1 milliradian goal after cycling. The tests also show that the nominal radius of both panels is smaller after cycling. This goes against the theory of thermal creep and its source is unknown.

Panels 1 and 2 were built to be delivered to NASA with no environmental cycling. We did however, measure the panels before and after coating to determine what effect the coating and glow discharge cleaning had on the radius. Pre coat measurement of the radius of curvature was made with a spherometer which mechanically measures the curvature without requiring a reflective surface. The post coat test were made with the test station described above. Again, the tests indicate a relaxation flattening during the coating / cleaning process but not as severe as for panels A, B, or C.

VI. CONCLUSIONS

The analyses and tests performed have led to a panel design which initially appeared to be well suited to space operation. Repeated thermal cycle testing as well as one-time exposure to elevated temperatures during the coating process have indicated an instability in radius of curvature. Since a solar concentrator will require a stable curvature to focus properly this point makes the design, as described, unsuitable.

Although the final panel design proved unsuitable, several important results have come from this study. First, because the low operating temperature will promote contamination of the reflector through condensation, second surface reflectors (coating on back of glass) should probably not be pursued further. Second, thermal control coatings on the back of the panel have the potential to effectively control average operating temperature. Third, the basic glass-on-composite approach has the potential to provide a smooth reflector surface whose properties are not degraded from thermal cycling. However, further work is needed to solve the radius of curvature stability issue.

COMPONENT	THICKNESS (INCH)	AREA DENSITY (LBM/SQ FT)
SODA LIME GLASS FACESHEET	0.009	0.135
ALUMINUM COATING (2000A)	0.000008	---
FM73 FILM + 2-PLY 120 KEVLAR	0.007	0.07
EPOXY	0.0025	0.015
HONEYCOMB (0.0035 X 0.250 HEX)	0.24	0.067
EPOXY	0.0025	0.015
2-PLY 120 KEVLAR PREPREG	0.007	0.052
	-----	-----
TOTALS:	0.268008	0.354

Table 1. Generic design honeycomb panel construction used for thermal analyses. Properties shown are 'typical' and representative of the expected final design.

RADIATION PROPERTIES

LOCATION	SOLAR ABSORPTANCE	INFRARED EMITTANCE
GLASS (BACK-ALUMINIZED)	0.03	0.75
BACK ALUMINUM COATING	0.07	--
FRONT ALUMINUM COATING	0.10	0.048
KEVLAR INNER SURFACES	--	0.90
REAR KEVLAR FACESHEET OUTER SURFACE	--	0.01 TO 1.0 (AS NOTED)

THERMAL CONDUCTIVITIES

MATERIAL	CONDUCTIVITY (BTU FT/HR SQ-FT F)
SODA LIME GLASS FACESHEET	0.55
KEVLAR, STYLE 120 (PARALLEL)	0.525
KEVLAR, STYLE 120 (PERPENDICULAR)	0.124
ALUMINUM COATING	130

Table 2. Thermal analysis assumptions (properties). Material and surface properties are 'typical' values selected for analysis purposes in the absense of a point design.

	precoat	pre-cycling		post cycling	
	radius	radius	slope error	radius	slope error
A	n/a	27.9 M	0.62 mRad	n/a	n/a
B	n/a	25.2 M	0.69 mRad	20.7 M	0.72 mRad
C	n/a	40.8 M	0.60 mRad	25.6 M	0.67 mRad
1	10.4 M	11.1 M	0.61 mRad	n/a	n/a
2	9.1 M	13.5 M	0.58 mRad	n/a	n/a

Table 3. Pre- and post- thermal cycling radius and slope measurement results for spherical panels. Panels A, 1, and 2 were not thermally cycled. Panels B and C were thermally cycled.

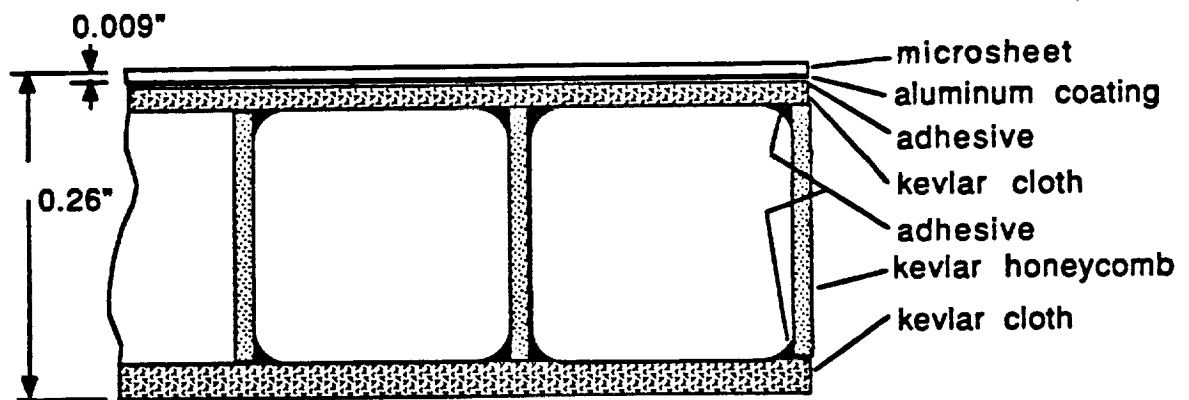


Figure 1. Baseline panel design using epoxy-bonded Kevlar substrate and Microsheet glass.

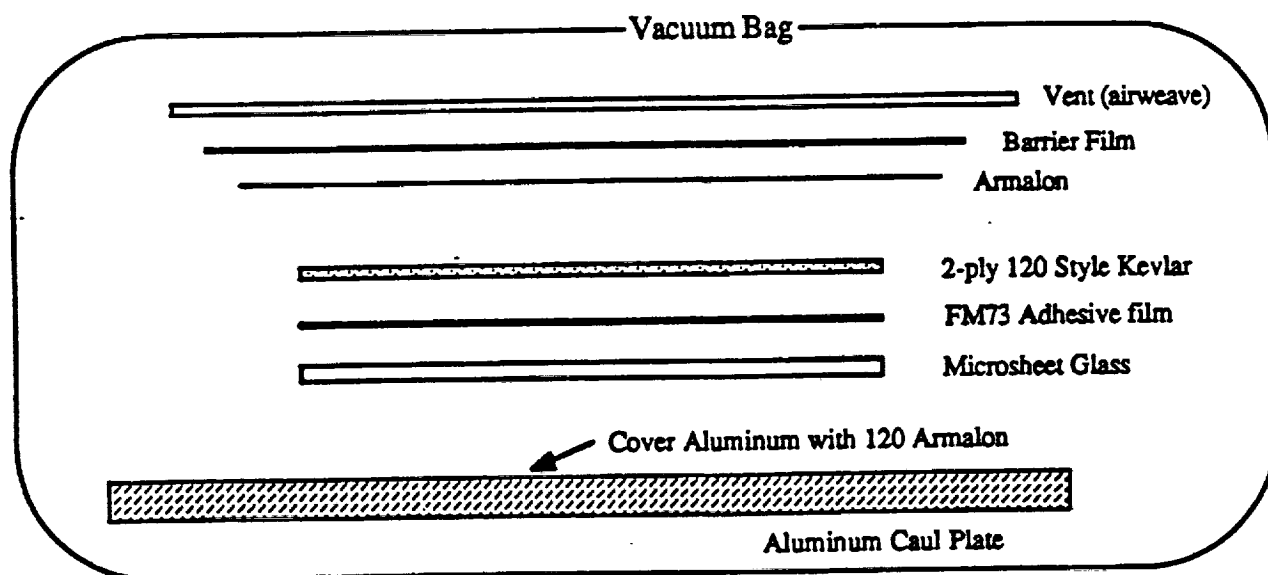


Figure 2. Typical glass - composite facesheet lamination sequence. Layup shown is for the Kevlar design. Process is similar for other materials.

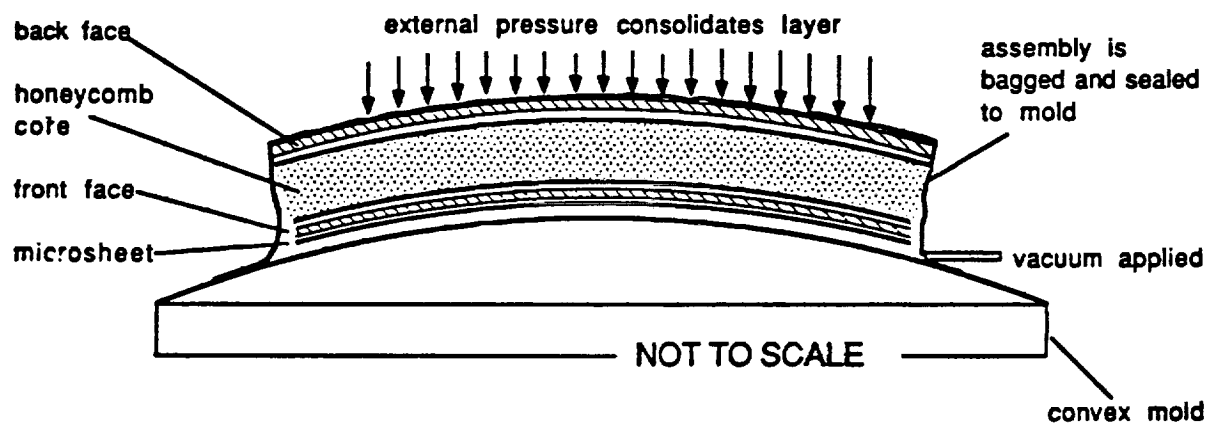


Figure 3. Typical panel assembly sequence. Panels are formed over a convex mold under vacuum and external pressure.

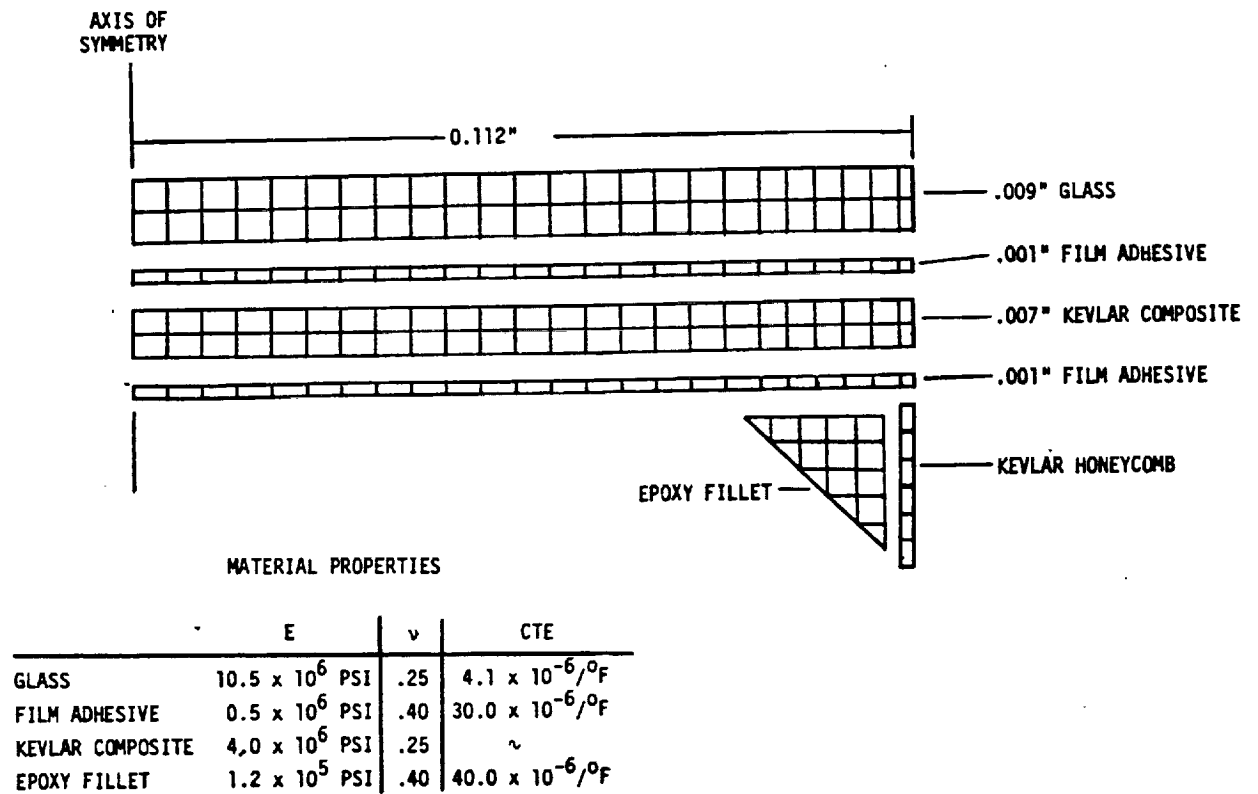


Figure 5. Unit cell model for analysis of structural behavior

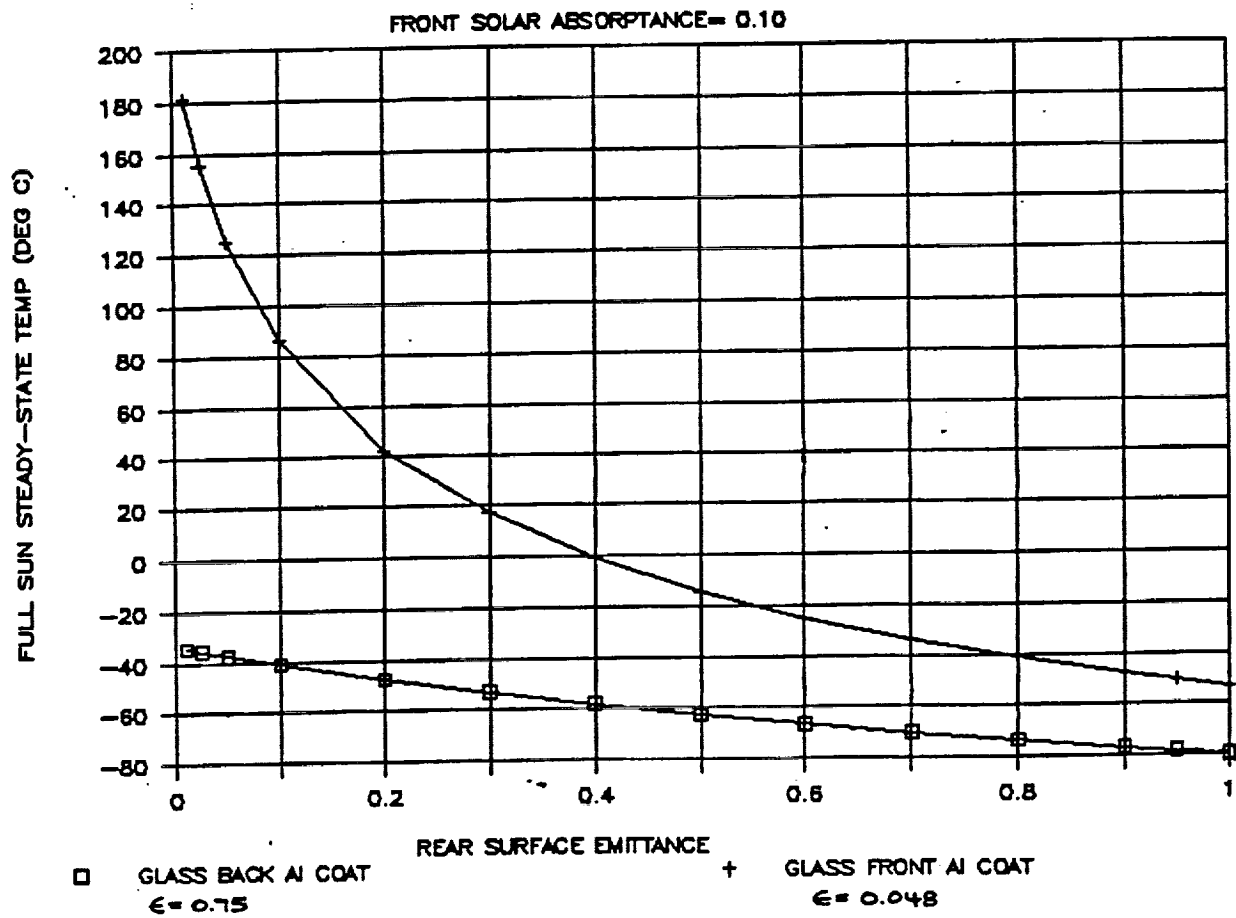


Figure 6. Effect of reflective film location on average steady state panel temperatures. First surface reflector has low emissivity, second surface reflector has high emissivity.

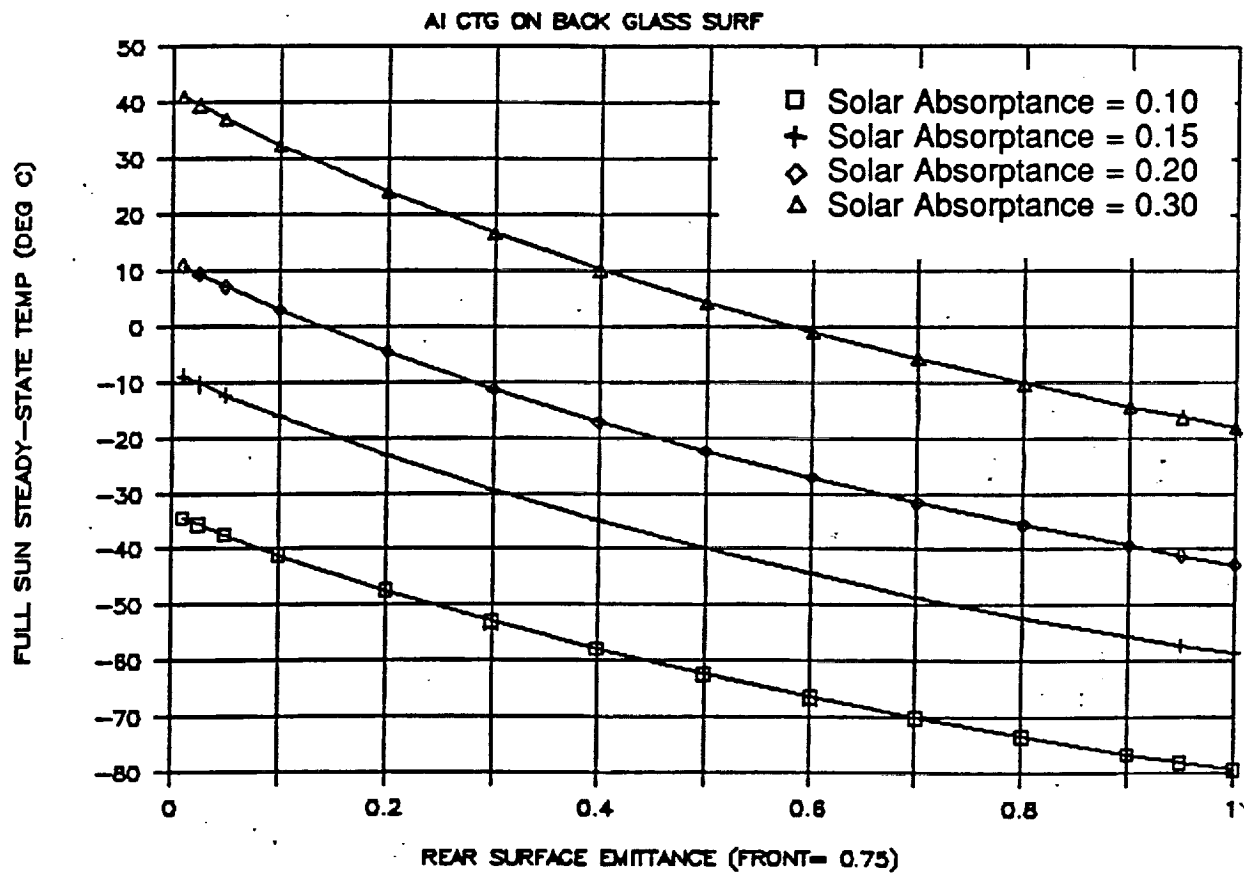


Figure 7. Effect of rear surface emittance on average steady state panel temperatures for back-coated face sheet.

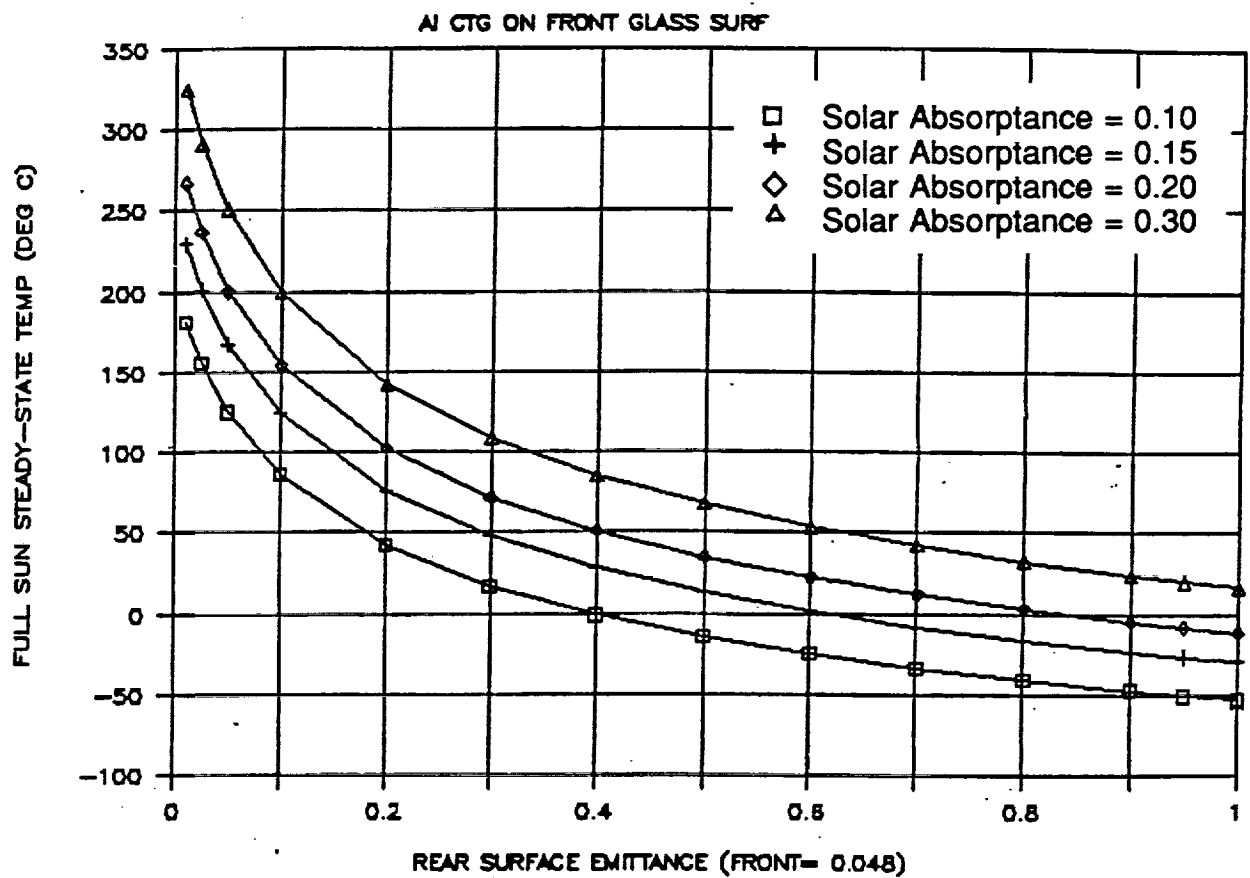


Figure 8. Effect of rear surface emissivity on steady state panel temperatures for front-coated facesheet.

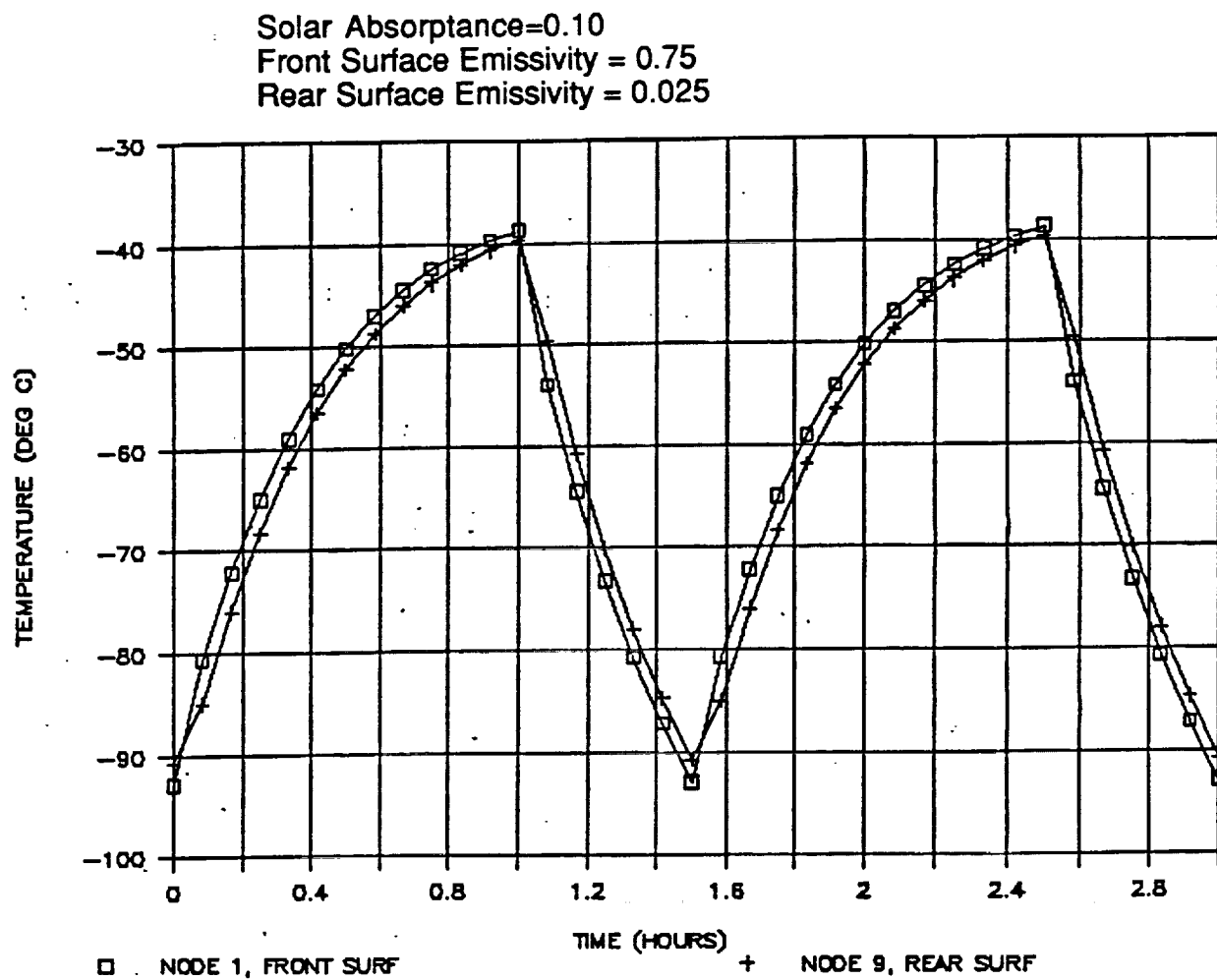


Figure 9. Orbital transient panel temperatures for back-coated glass

Solar Absorptance=0.10
 Front Surface Emissivity = 0.048
 Rear Surface Emissivity = 0.025

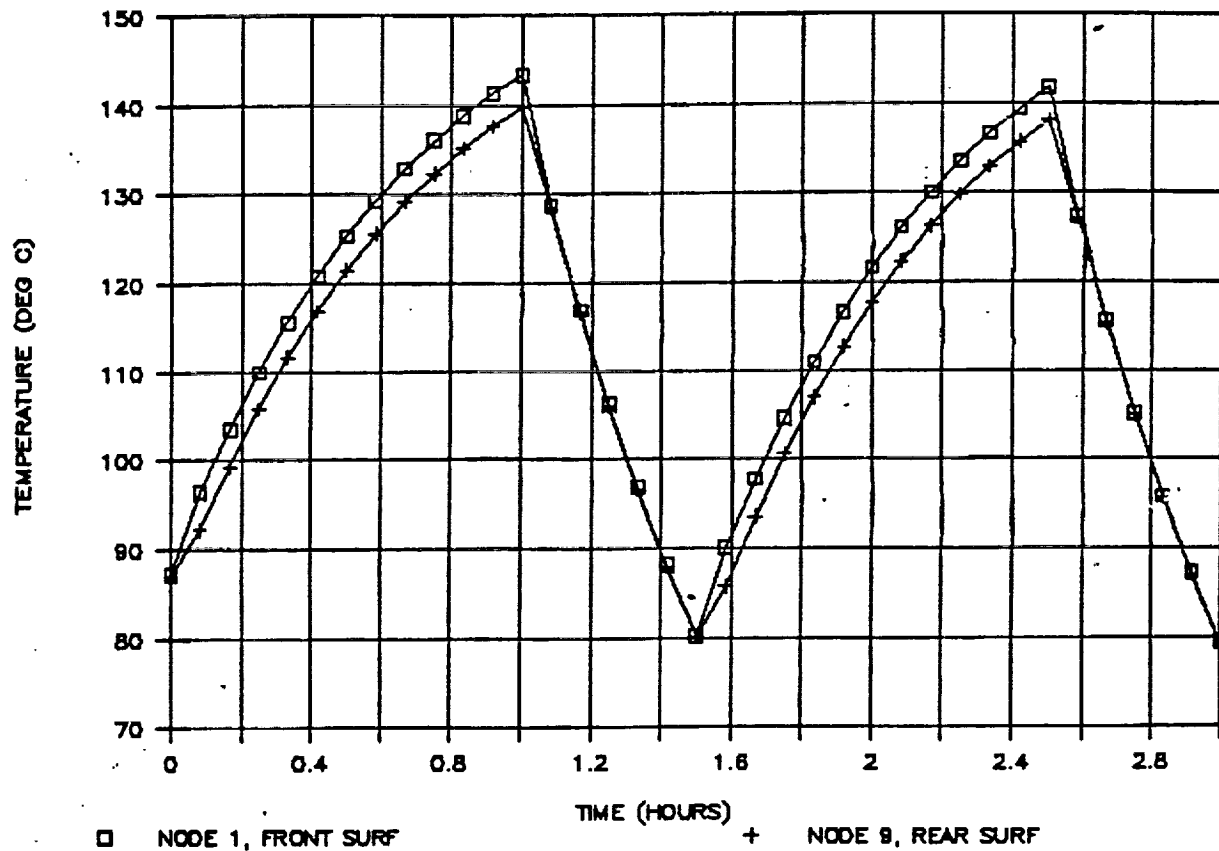


Figure 10. Orbital transient panel temperatures for front-coated glass

Solar Absorptance=0.10
Front Surface Emissivity = 0.75
Rear Surface Emissivity = 0.025

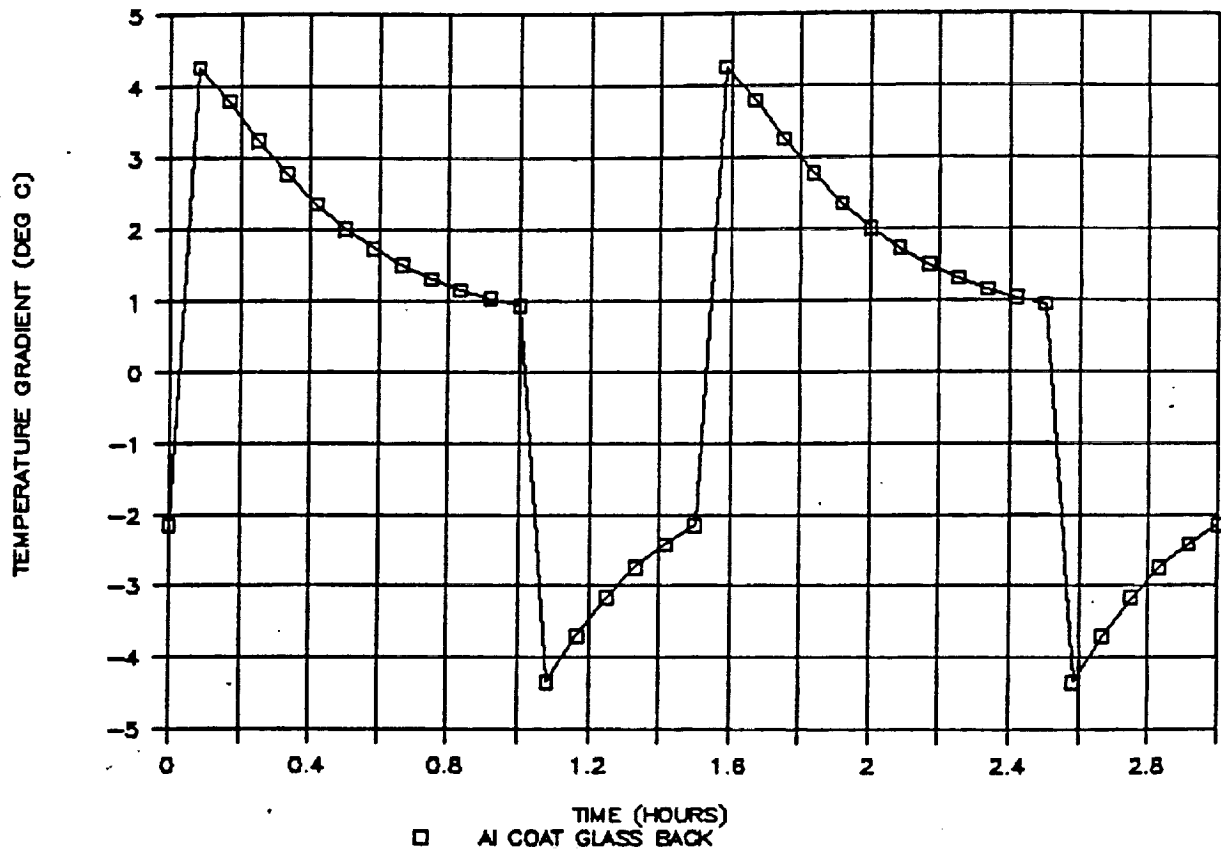


Figure 11. Front-to-back temperature gradient for back-coated panel

Solar Absorptance=0.10
Front Surface Emissivity = 0.048
Rear Surface Emissivity = 0.025

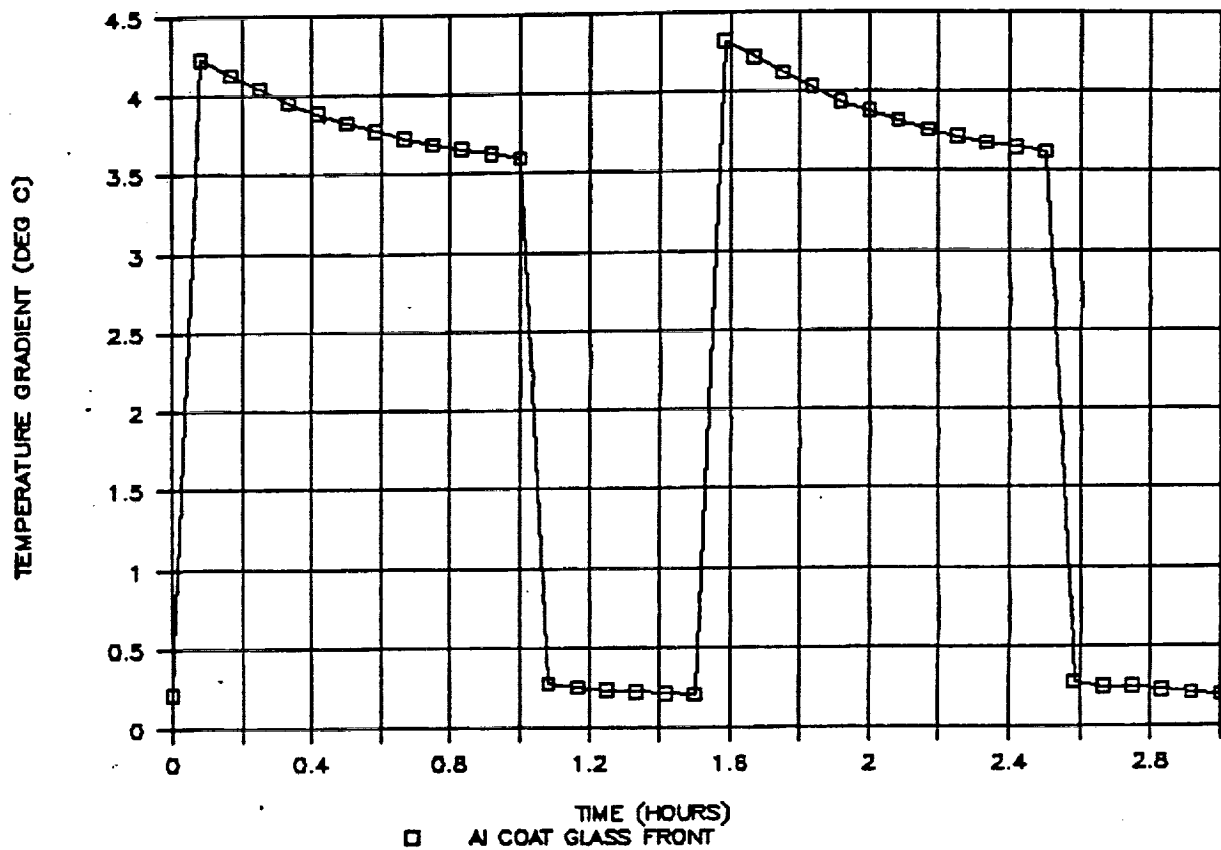


Figure 12. Front-to-back temperature gradient for front-coated panel

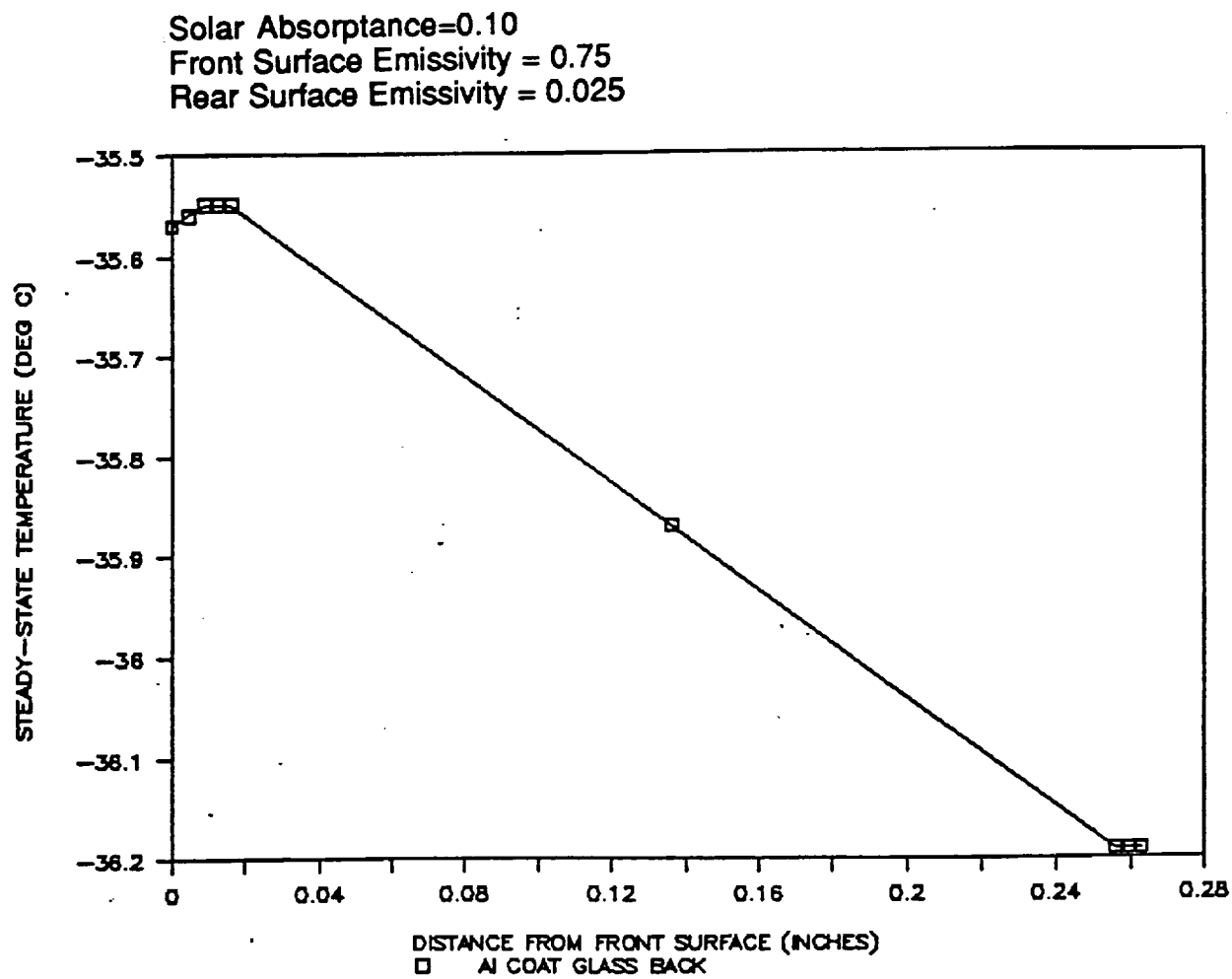


Figure 13. Through the thickness temperatures for back-coated panel

Solar Absorptance=0.10
Front Surface Emissivity = 0.048
Rear Surface Emissivity = 0.025

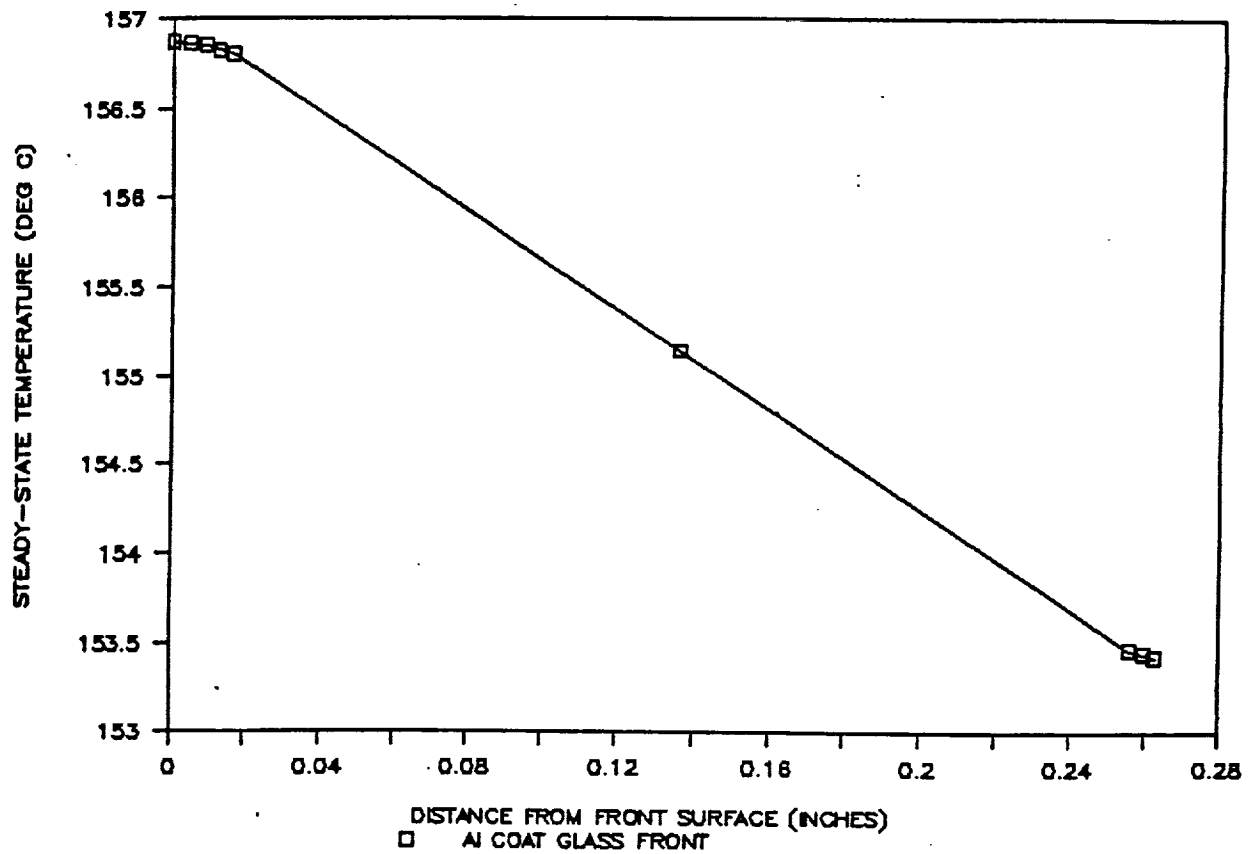


Figure 14. Through the thickness temperatures for front-coated panel

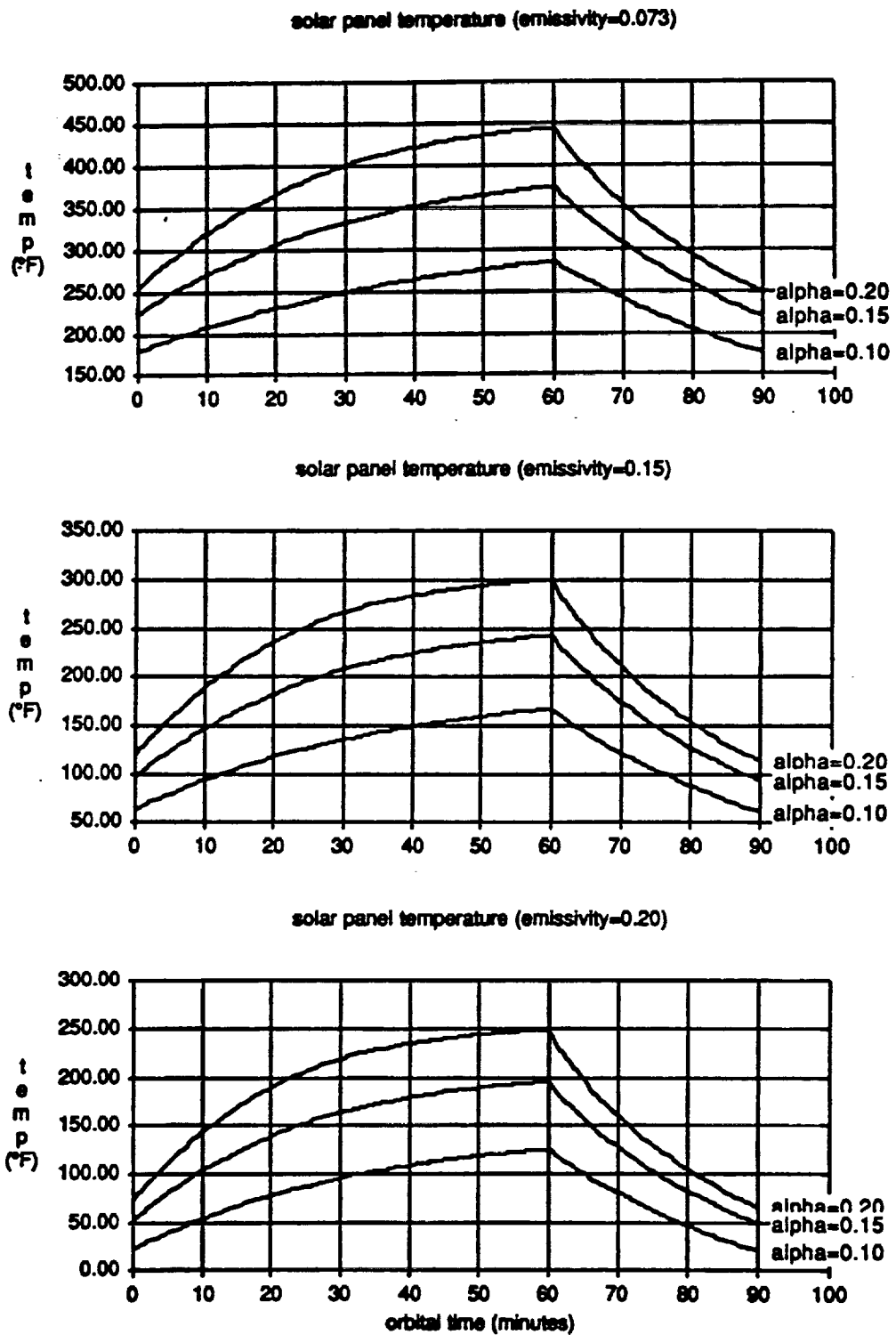


Figure 15. Orbital transient panel temperatures as a function of total surface emissivity using closed form analysis

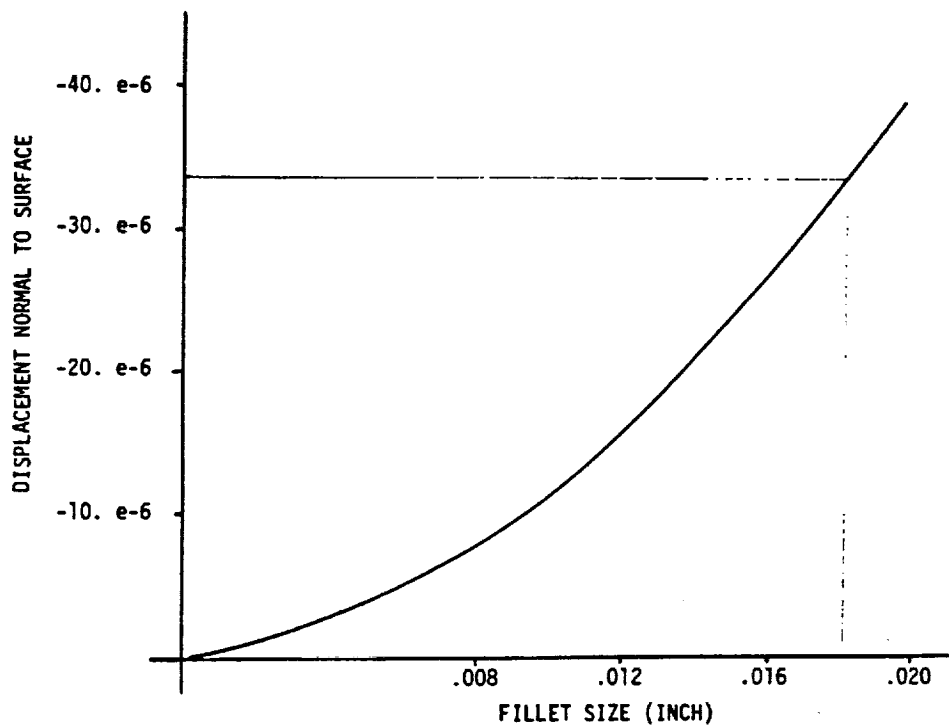


Figure 16. Effect of adhesive fillet size on panel surface deformations (peak) for an adhesive cure shrinkage rate of 1/2% linear.

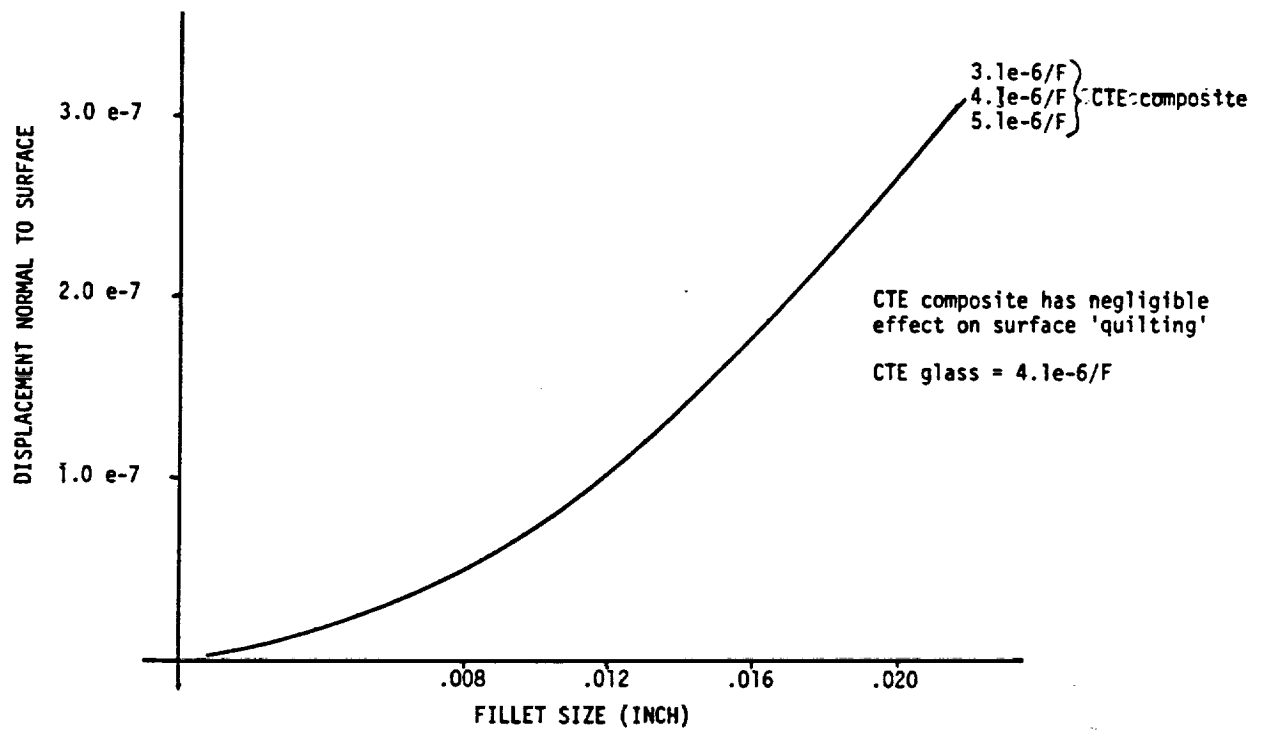


Figure 17. Effect of adhesive fillet size on panel surface quilting deformations (peak) for a temperature change of 1°F .

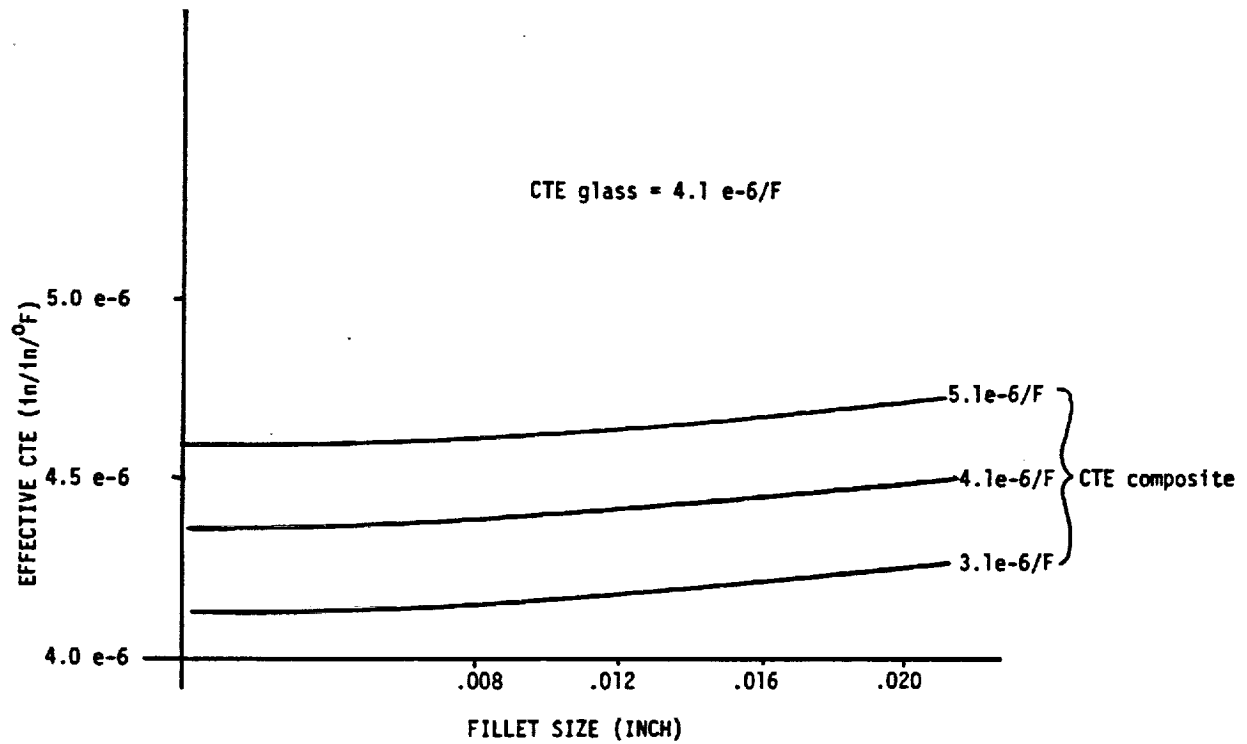


Figure 18. Effect of adhesive fillet size on facesheet 'effective CTE' as a function of fillet size and substrate CTE.

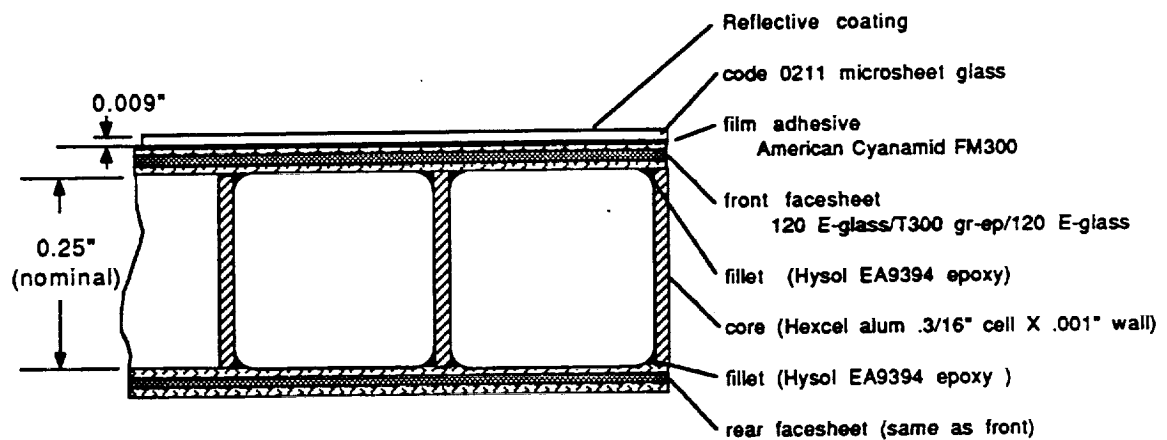


Figure 19. Point design description resulting from thermal and structural analyses.

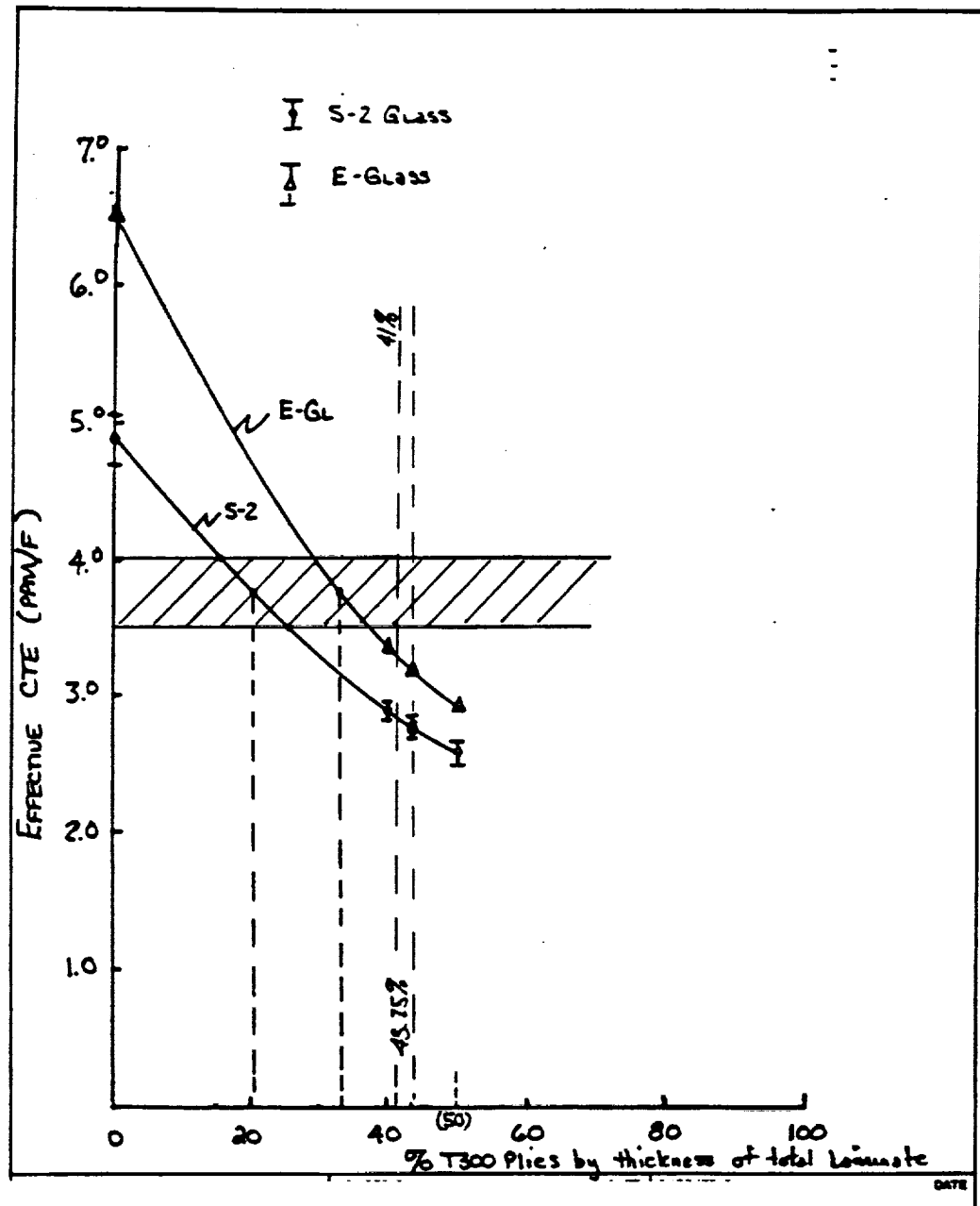


Figure 20. Design of composite laminate to match required CTE

- CTE of 3 coupon substrates measured between -100 and 200 °F
- 4.0, 4.54, and 4.36 ppm/°F measured
- Resultant CTE's acceptable.

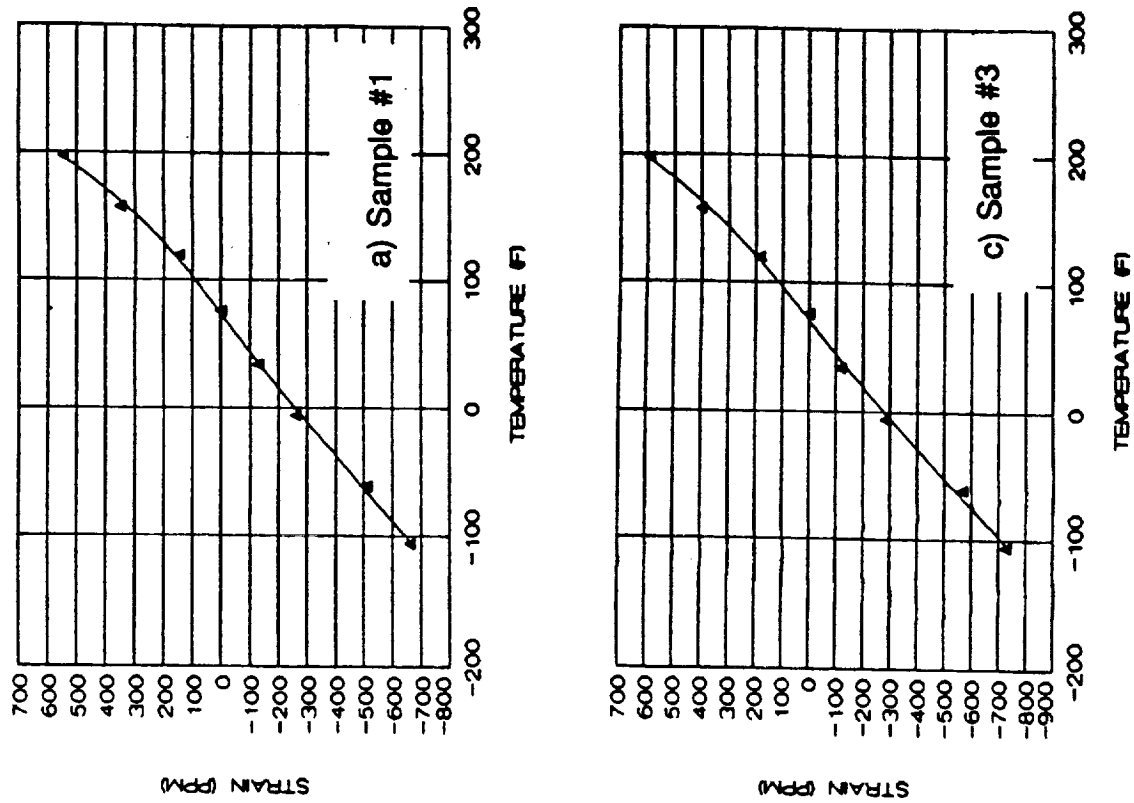


Figure 21. Coupon tests of substrate CTE for chosen laminate design

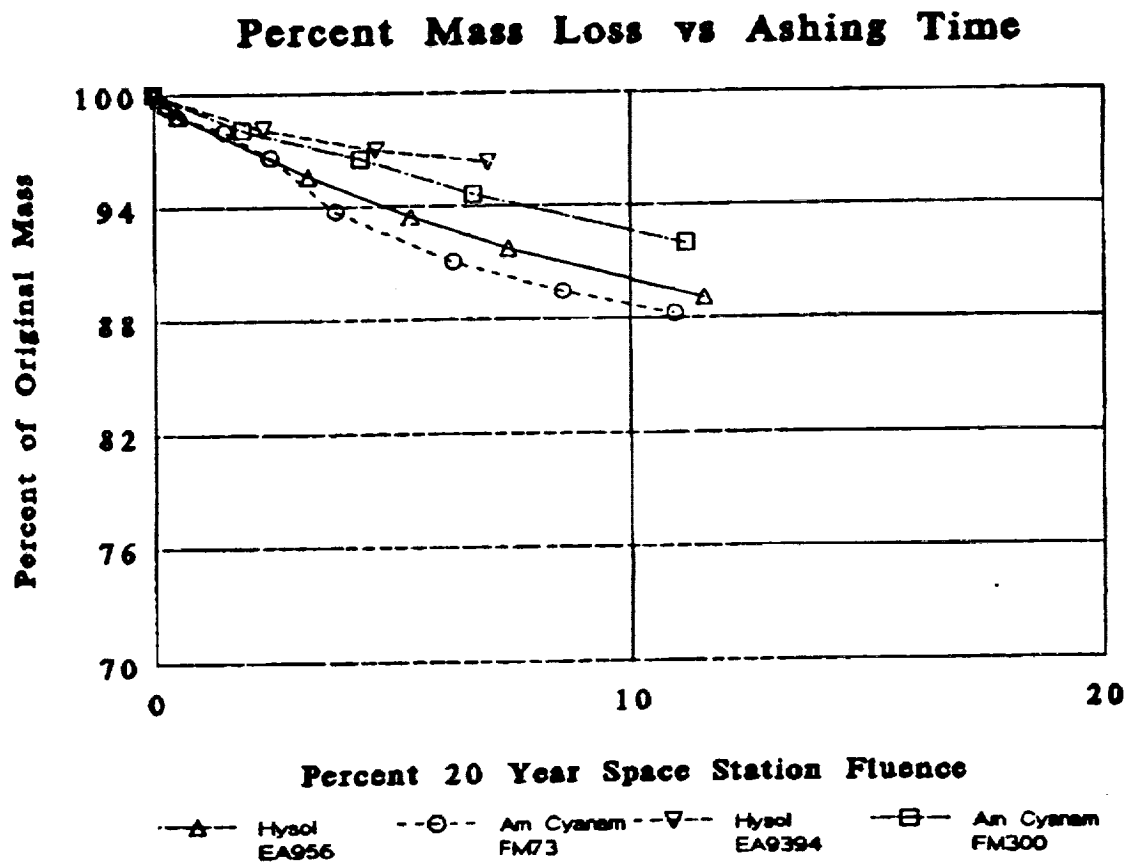
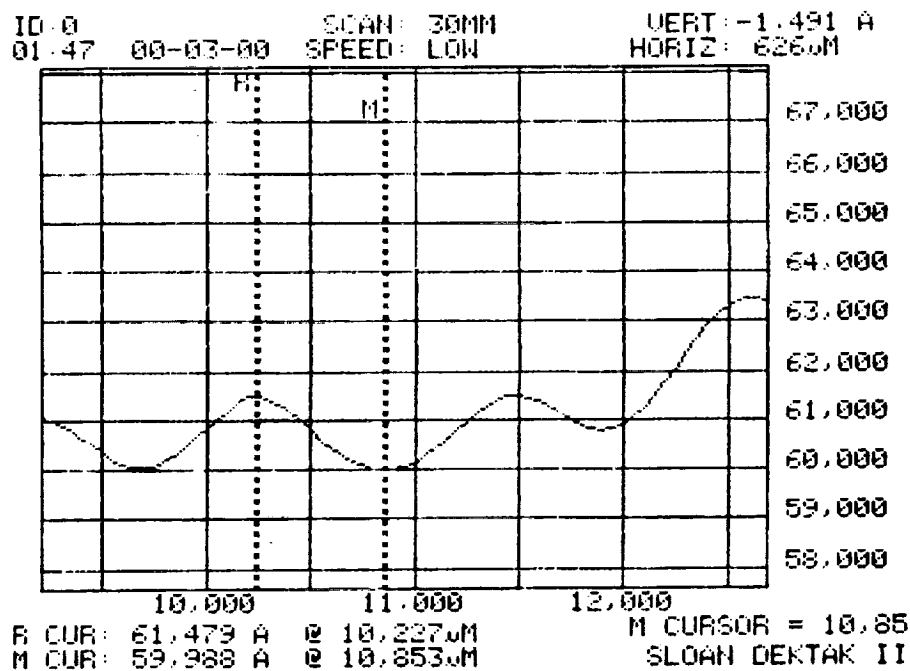
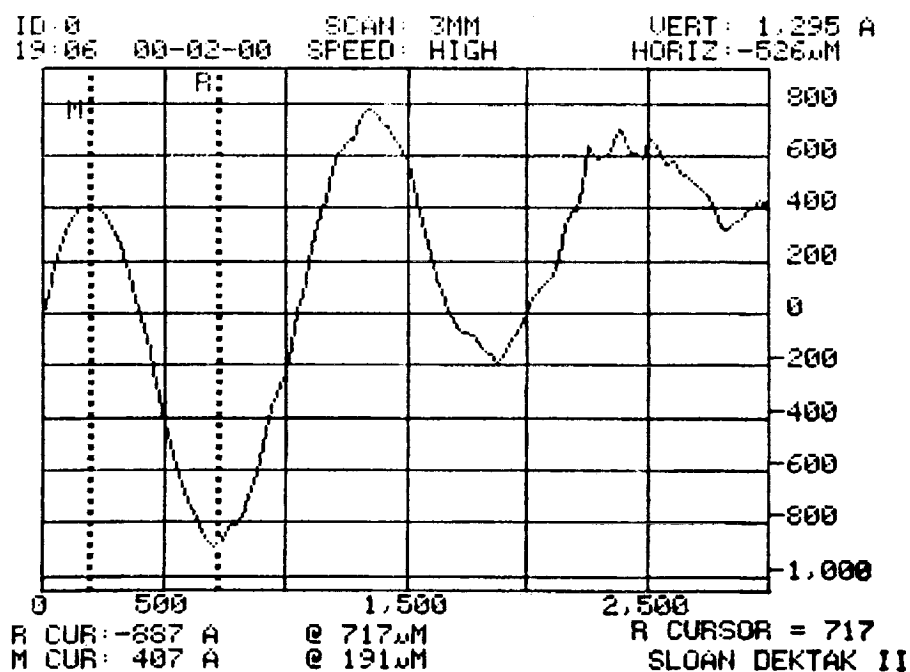


Figure 22. Atomic oxygen erosion tests of candidate adhesives



Before



After

Figure 23. Coupon surface distortion before and after thermal cycling. Surface height (vertical) measured in Angstroms, surface span (horizontal) is microns.

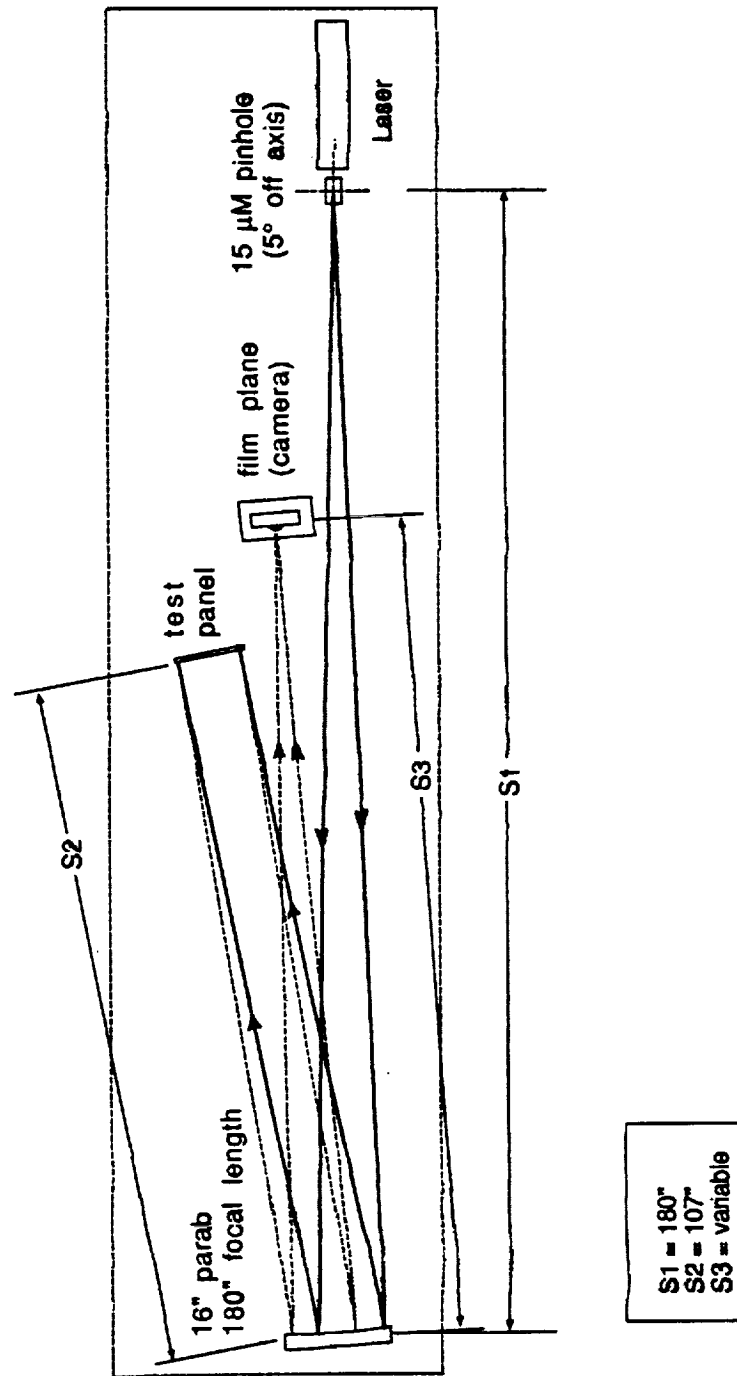


Figure 24. Diagram of test station to measure radius of curvature and integrated (rms) slope error of spherical test panels.

TEST ID - MIRROR A X-SCAN DATE 01/25/90

DENSITY - DIFFUSE

PTS/SCAN 261

SCAN APERTURE 30.0 MICROMETER

SAMPLING INCR 200.00 MICROMETER

TAPE NUMBER 109

PATTERN - 01.0

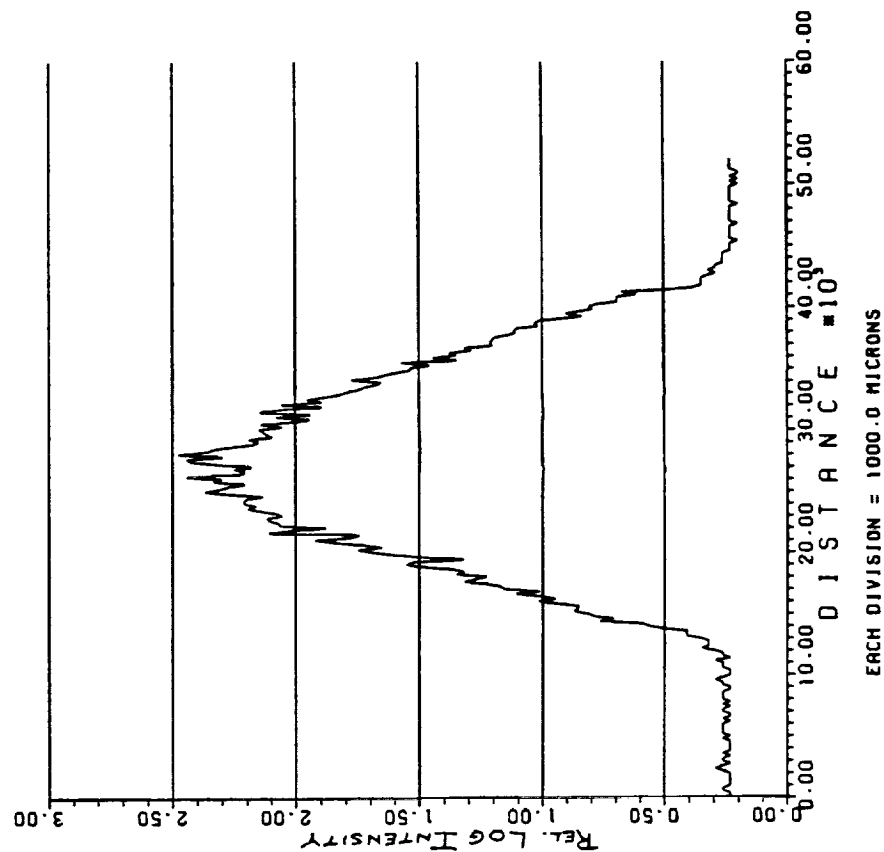
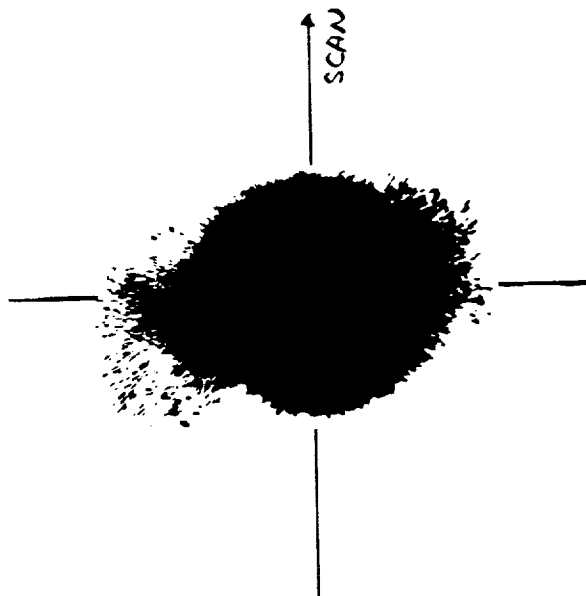


Figure 25. Typical image spot from spherical panel and intensity scan

LIST of REFERENCES

1. Rockwell, R., "Lightweight Solar Concentrator Panel for Space Applications", NASA CR-180894, July 1988
2. Gulino, D., "Atomic-Oxygen Durability of Impact-Damaged Solar Reflectors" Journal of Spacecraft, Vol 25, No 1, Feb 1988
3. Richter, S. and Lacey, D., "Technology Development Program for an Advanced Microsheet Glass Concentrator", 1990 International Solar Energy Conference sponsored by the American Society of Mechanical Engineers, April 1990

REPORT DOCUMENTATION PAGE			Form Approved OMB No. 0704-0188	
Public reporting burden for this collection of information is estimated to average 1 hour per response, including the time for reviewing instructions, searching existing data sources, gathering and maintaining the data needed, and completing and reviewing the collection of information. Send comments regarding this burden estimate or any other aspect of this collection of information, including suggestions for reducing this burden, to Washington Headquarters Services, Directorate for Information Operations and Reports, 1215 Jefferson Davis Highway, Suite 1204, Arlington, VA 22202-4302, and to the Office of Management and Budget, Paperwork Reduction Project (0704-0188), Washington, DC 20503.				
1. AGENCY USE ONLY (Leave blank)		2. REPORT DATE March 1993		3. REPORT TYPE AND DATES COVERED Final Contractor Report
4. TITLE AND SUBTITLE Solar Concentrators for Advanced Solar-Dynamic Power Systems in Space			5. FUNDING NUMBERS WU-506-41-31 C-NAS3-25280	
6. AUTHOR(S) Richard Rockwell				
7. PERFORMING ORGANIZATION NAME(S) AND ADDRESS(ES) Hughes Danbury Optical Systems, Inc. 100 Wooster Heights Road Danbury, Connecticut 06810-7589			8. PERFORMING ORGANIZATION REPORT NUMBER E-7712	
9. SPONSORING/MONITORING AGENCY NAMES(S) AND ADDRESS(ES) National Aeronautics and Space Administration Lewis Research Center Cleveland, Ohio 44135-3191			10. SPONSORING/MONITORING AGENCY REPORT NUMBER NASA CR-187148	
11. SUPPLEMENTARY NOTES Project Manager, T.S. Mroz, (216) 433-6168.				
12a. DISTRIBUTION/AVAILABILITY STATEMENT Unclassified - Unlimited Subject Category 20			12b. DISTRIBUTION CODE	
13. ABSTRACT (Maximum 200 words) This report summarizes the results of a study performed by Hughes Danbury Optical Systems, HDOS, (formerly Perkin-Elmer) to design, fabricate, and test a lightweight (2 kg/sq M), self supporting, and highly reflective sub-scale concentrating mirror panel suitable for use in space. The HDOS panel design utilizes Corning's "microsheet" glass as the top layer of a composite honeycomb sandwich. This approach, whose manufacturability was previously demonstrated under an earlier NASA contract, provides a smooth (specular) reflective surface without the weight of a conventional glass panel. The primary result of this study is a point design and it's performance assessment.				
14. SUBJECT TERMS Solar concentrator; Microsheet; Fabrication			15. NUMBER OF PAGES 50	
			16. PRICE CODE A03	
17. SECURITY CLASSIFICATION OF REPORT Unclassified	18. SECURITY CLASSIFICATION OF THIS PAGE Unclassified	19. SECURITY CLASSIFICATION OF ABSTRACT Unclassified	20. LIMITATION OF ABSTRACT	